Quantum Tunneling Analog of Black Hole Thermodynamics via Fermion-Photon Confined Spectra

Travis S. Taylor[1,2]

[1]QuantumFrontier, LLC, Huntsville, AL, USA.
[2]Department of Physics, University of Alabama in Huntsville, AL, USA.
E-mail: tst0072@uah.edu

We introduce a quantum mechanical model that reproduces key thermodynamic features of a Schwarzschild black hole using a spherical finite potential well. By analyzing the tunneling spectra of photons and fermions confined in this well, we demonstrate a numerical match to Hawking radiation. Additionally, the entropy of the emitted spectrum exhibits a geometric scaling consistent with the Bekenstein-Hawking formula. These results suggest that quantum confinement may serve as an analog platform for exploring black hole thermodynamics.

1 Introduction

This study highlights a formal similarity between quantum mechanical tunneling and gravitational radiation processes, suggesting a deeper, underlying unity between quantum confinement and curved spacetime thermodynamics. The findings propose potential insights into the quantum mechanical underpinnings of black hole thermodynamics and contribute to the ongoing dialogue on the unification of quantum mechanics and general relativity.

Black holes, as described by general relativity, exhibit thermodynamic properties such as Hawking radiation and entropy, hinting at a quantum mechanical foundation [1]. This study develops a three-dimensional spherical quantum well model with a finite potential barrier to explore these properties under controlled conditions.

This work departs from prior analog black hole models by constructing a purely quantum mechanical system that, when scaled appropriately, numerically reproduces the full Hawking spectrum. In contrast to acoustic or optical analogs, our approach uses tunneling in a finite spherical well to model both bosonic and fermionic emission spectra and entropy, providing a unified thermal analog of black hole radiation. The model's ability to quantitatively match the black hole spectrum across a wide frequency range, using temperature scaling and statistical blending, demonstrates a deeper thermodynamic equivalence rooted in quantum confinement rather than relativistic curvature.

Unlike analog gravity models based on fluid flow or optical horizons [2, 3], this approach relies purely on quantum mechanical tunneling in a finite potential structure. We begin by formulating a spherical quantum well model with a barrier structure mimicking an event horizon. Photon and fermion spectra are then derived using WKB approximations, and the resulting emission profiles are compared to Hawking radiation. We also compute entropy scaling and propose a dimensionless scaling relation that aligns the two systems thermodynamically.

2 Background

2.1 Schwarzschild black holes and event horizon

A Schwarzschild black hole, a spherically symmetric, nonrotating solution to Einstein's field equations, is characterized by the metric [4, 5]:

$$ds^2 = -\left(1 - \frac{2GM}{c^2 r}\right)c^2 dt^2 + \left(1 - \frac{2GM}{c^2 r}\right)^{-1} dr^2 + r^2\left(d\theta^2 + \sin^2\theta\, d\phi^2\right), \quad (1)$$

where G is the gravitational constant, M is the mass, c is the speed of light, r is the radial coordinate, t is time, and θ, ϕ are angular coordinates. The event horizon, at the Schwarzschild radius:

$$R_s = \frac{2GM}{c^2}, \quad (2)$$

marks the boundary where escape velocity equals c, rendering escape impossible classically. Hawking radiation, a quantum phenomenon, suggests black holes emit thermal radiation at temperature $T_H = \frac{\hbar c^3}{8\pi GMk_B}$ [1].

2.2 The 3D finite quantum well

In quantum mechanics, a finite spherical well confines particles with a potential [6]:

$$V(r) = \begin{cases} 0 & \text{for } r < R_s \\ V_0\, e^{-\lambda(r-R_s)} & \text{for } R_s \leqslant r < R \\ V_1\, e^{-\lambda(r-R)} & \text{for } r \geqslant R \end{cases} \quad (3)$$

where V_0 (in eV) is the barrier height, $V_1 < V_0$ is the exterior potential, R is the outer radius, and λ (in m^{-1}) controls decay. Unlike infinite wells, this permits tunneling, a key feature in semiconductor applications [7] (see Figure 1).

2.3 Event horizons and barriers

The black hole event horizon and quantum well barrier both define boundaries, but differ fundamentally. The horizon requires infinite energy for escape, per general relativity, while

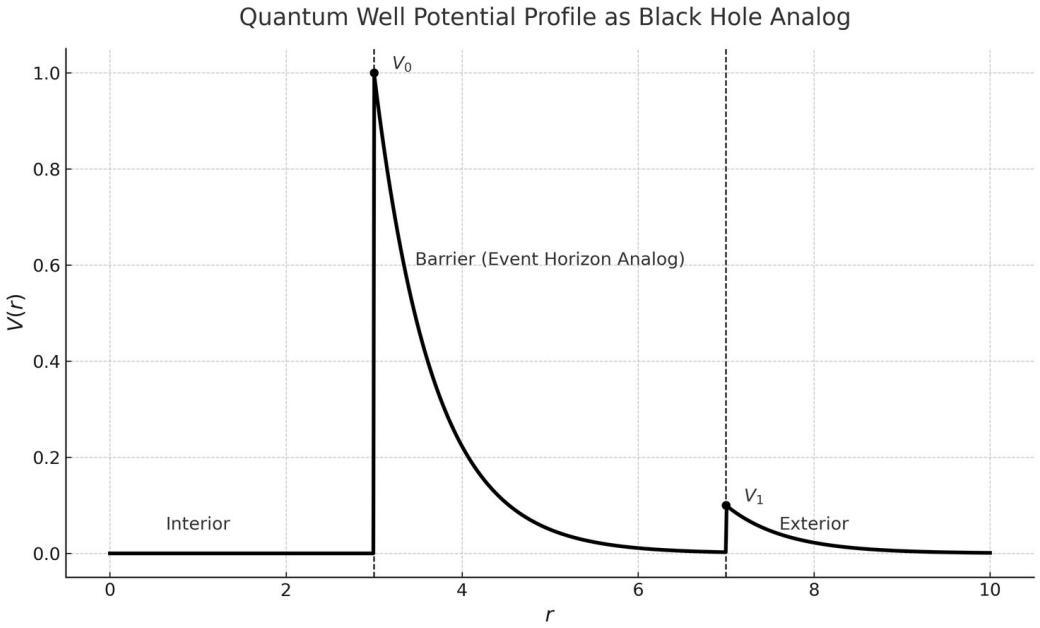

Fig. 1: Radial potential profile $V(r)$ illustrating the structure of the spherical quantum well. The barrier begins at R_s with height V_0 and decays exponentially toward V_1 by radius R. Regions labeled: Interior ($r < R_s$), Barrier (Event Horizon Analog, $R_s < r < R$), and Exterior ($r > R$).

the quantum barrier allows probabilistic tunneling [6]. This contrast highlights deterministic versus probabilistic physics, yet both systems suggest a transition from confinement to escape, inspiring our analogy.

3 Quantum well model formulation

3.1 Quantum well model setup

Our quantum well is a spherical system with potential:

$$V(r) = \begin{cases} 0 & \text{for } r < R_s \\ V_0\, e^{-\lambda(r-R_s)} & \text{for } R_s \leqslant r < R \\ V_1\, e^{-\lambda(r-R)} & \text{for } r \geqslant R \end{cases} \tag{4}$$

where $R_s = \frac{2GM}{c^2}$ aligns with the Schwarzschild radius, V_0 sets the barrier, and λ emulates gravitational decay. This structure includes an interior ($r < R_s$), a transition region ($R_s \leqslant r < R$), and an exterior ($r \geqslant R$), mirroring a black hole's zones.

To rigorously establish the energy spectrum and tunneling behavior of the quantum well, we solve the time-independent Schrödinger equation:

$$-\frac{\hbar^2}{2m}\,\nabla^2\psi + V(r)\psi = E\psi\,. \tag{5}$$

Expanding in spherical coordinates and assuming a separable solution $\psi(r,\theta,\phi) = R(r)\,Y_l^m(\theta,\phi)$, the radial equation becomes:

$$\frac{d^2R}{dr^2} + \frac{2}{r}\frac{dR}{dr} + \left[\frac{2m}{\hbar^2}\,(E - V(r)) - \frac{l(l+1)}{r^2}\right]R = 0\,. \tag{6}$$

We solve this equation in three regions: (i) inside the well ($r < R_s$), (ii) within the barrier ($R_s \leqslant r < R$), and (iii) outside the well ($r > R$).

The full wavefunction $\psi(r,\theta,\phi)$ is continuous and differentiable across region boundaries at $r = R_s$ and $r = R$, requiring matching of both the radial function and its derivative:

$$R_{\text{in}}(R_s) = R_{\text{barrier}}(R_s)\,, \quad R'_{\text{in}}(R_s) = R'_{\text{barrier}}(R_s)\,, \tag{7}$$

$$R_{\text{barrier}}(R) = R_{\text{out}}(R)\,, \quad R'_{\text{barrier}}(R) = R'_{\text{out}}(R)\,. \tag{8}$$

These boundary conditions yield a transcendental equation for energy levels E_n, which must be solved numerically.

In practice, these are implemented using numerical shooting methods or root-finding on determinant conditions from matched solutions [8].

3.2 Inside the well region ($r < R_s$)

For a potential well with $V(r) = 0$, the equation simplifies to:

$$\frac{d^2R}{dr^2} + \frac{2}{r}\frac{dR}{dr} + \left(k^2 - \frac{l(l+1)}{r^2}\right)R = 0\,, \tag{9}$$

where $k^2 = \frac{2mE}{\hbar^2}$. The general solution in this region is given by the spherical Bessel function:

$$R_{\text{in}}(r) = A\, j_l(kr)\,, \tag{10}$$

where $j_l(x)$ is the spherical Bessel function of the first kind.

3.3 Barrier region: ($R_s \leqslant r < R$)

In the barrier region, the potential is modeled as an exponentially decaying function:

$$V(r) = V_0\, e^{-\lambda(r-R_s)}. \tag{11}$$

The Schrödinger equation in this region is:

$$\frac{d^2R}{dr^2} + \frac{2}{r}\frac{dR}{dr} + \left[\frac{2m}{\hbar^2}(E - V_0\, e^{-\lambda(r-R_s)}) - \frac{l(l+1)}{r^2}\right]R = 0. \tag{12}$$

Since this equation does not have a simple analytic solution, we apply the Wentzel-Kramers-Brillouin (WKB) approximation to estimate the tunneling probability [9]:

$$T(E) \approx e^{-2\int_{R_s}^{R}\sqrt{\frac{2m}{\hbar^2}(V(r)-E)}\,dr}. \tag{13}$$

For classically forbidden regions where $E < V(r)$, the wavefunction exhibits exponential decay:

$$R_{\text{barrier}}(r) \approx Ce^{-\frac{\sqrt{2mV_0}}{\hbar\lambda}e^{-\lambda(r-R_s)}}. \tag{14}$$

3.4 Outside the well ($r > R$)

For large r, we assume the potential is negligible, and the Schrödinger equation reduces to:

$$\frac{d^2R}{dr^2} + \frac{2}{r}\frac{dR}{dr} + \left(k_0^2 - \frac{l(l+1)}{r^2}\right)R = 0, \tag{15}$$

where $k_0^2 = \frac{2m(E-V_1)}{\hbar^2}$. The general solution for outgoing waves is given by the spherical Hankel function:

$$R_{\text{out}}(r) = Bh_l^{(1)}(k_0 r), \tag{16}$$

where $h_l^{(1)}(x)$ represents the spherical Hankel function of the first kind.

3.5 Matching conditions and energy quantization

The wavefunction and its derivative must be continuous at $r = R_s$ and $r = R$:

$$R_{\text{in}}(R_s) = R_{\text{barrier}}(R_s), \quad R'_{\text{in}}(R_s) = R'_{\text{barrier}}(R_s), \tag{17}$$

$$R_{\text{barrier}}(R) = R_{\text{out}}(R), \quad R'_{\text{barrier}}(R) = R'_{\text{out}}(R). \tag{18}$$

These conditions yield a transcendental equation that determines the allowed energy levels E_n, which must be solved numerically. By solving the Schrödinger equation in each region and applying boundary conditions, we obtain the wavefunctions and energy levels for the quantum well. The WKB approximation provides an estimate for the tunneling probability, supporting the interpretation that the system exhibits black hole-like emission characteristics.

For a potential of the form $V(r) = V_0\, e^{-\lambda(r-R_s)}$, the classical turning points r_1, r_2 are defined by $V(r) = E$, yielding:

$$r_2 - R_s = \frac{1}{\lambda}\ln\left(\frac{V_0}{E}\right), \quad r_1 = R_s.$$

Hence, the WKB tunneling probability is:

$$T(E) \approx \exp\left[-\frac{2}{\hbar}\int_{R_s}^{r_2}\sqrt{2m(V(r)-E)}\,dr\right]. \tag{19}$$

4 Energy quantization and photon statistics

Photons in the well follow the Helmholtz equation [6]:

$$\left[\frac{d^2}{dr^2} + \frac{2}{r}\frac{d}{dr} - \frac{l(l+1)}{r^2} + k^2\right]R(r) = 0, \tag{20}$$

where $k = \frac{E}{\hbar c}$. The finite barrier allows tunneling, yielding approximate energies:

$$E_{nl} \approx \hbar c\,\frac{x_{nl}}{R}, \tag{21}$$

where x_{nl} adjusts for penetration.

The partition function for N photons, using Bose-Einstein statistics [10], is:

$$Z = \prod_{n,l}\left(\frac{1}{1 - e^{-\beta E_{nl}}}\right)^{2l+1}, \tag{22}$$

where $\beta = 1/(k_B T)$.

5 Calculation of internal energy

The internal energy is [10]:

$$E_{\text{int}} = -\frac{\partial \ln Z}{\partial \beta} = \sum_{n,l}(2l+1)\,E_{nl}\,\frac{1}{e^{\beta E_{nl}} - 1}. \tag{23}$$

The energy density per unit volume for blackbody photons confined in a spherical well of radius R is given by integrating over the Bose-Einstein distribution:

$$E_{\text{int}} = \int_0^\infty g(E)\,\frac{E}{e^{\beta E} - 1}\,dE \tag{24}$$

with $g(E) = \frac{8\pi R^3}{h^3c^3}E^2$, yielding:

$$E_{\text{int}} = \frac{8\pi R^3}{h^3c^3}\int_0^\infty \frac{E^3}{e^{\beta E} - 1}\,dE = \frac{8\pi^5 R^3 (k_B T)^4}{15\,h^3c^3}. \tag{25}$$

Assuming a dominant tunneling angular momentum mode $l = 1$, we multiply by the degeneracy $2l + 1 = 3$.

For a dominant $l_{\text{es}} = 1$, assumed as the primary tunneling mode for simplicity [6]:

$$E_{\text{int}} \approx 3\int_0^\infty \frac{8\pi R^3}{h^3c^3}\,E^3\,\frac{1}{e^{\beta E} - 1}\,dE = 3\frac{8\pi^5 R^3 (k_B T)^4}{15\,h^3c^3}, \tag{26}$$

using the photon density of states $g(E) = \frac{8\pi R^3}{h^3c^3}E^2$.

6 Emission spectra from quantum tunneling

The tunneled energy spectrum for photons escaping the quantum well is derived using the grand canonical ensemble and tunneling probability [11, 12]:

$$I_{\text{tunneled}}(E) = \frac{8\pi R^3}{h^3c^3}E^3\frac{T(E)}{e^{E/k_BT}-1}, \tag{27}$$

where $g(E) = \frac{8\pi R^3}{h^3c^3}E^2$ is the photon density of states, and $T(E)$ is the tunneling probability through the barrier $V(r) = V_0\,e^{-\lambda(r-R_s)}$ from R_s to R. For photons, the WKB approximation [9] gives:

$$T(E) = e^{-2\int_{R_s}^{R}\frac{\sqrt{V_0\,e^{-\lambda(r-R_s)}-E}}{\hbar c}\,dr}. \tag{28}$$

Substituting $u = r - R_s$, the energy-dependent tunneling probability is:

$$T(E) = e^{-\frac{2}{\hbar c}\int_0^{R-R_s}\sqrt{V_0\,e^{-\lambda u}-E}\,du}, \tag{29}$$

valid for $E < V_0\,e^{-\lambda(R-R_s)}$, where the integral modulates the spectrum as a transmission factor. An earlier approximation assuming $V_0\,e^{-\lambda(r-R_s)} \gg E$ yielded $T(E) \approx e^{-\frac{2\sqrt{V_0}}{\hbar c\lambda}(R-R_s)}$, but here we retain E-dependence for accuracy. The full spectrum becomes:

$$I_{\text{tunneled}}(E) = \frac{8\pi R^3}{h^3c^3}e^{-\frac{2}{\hbar c}\int_0^{R-R_s}\sqrt{V_0e^{-\lambda u}-E}\,du}\frac{E^3}{e^{E/k_BT}-1}. \tag{30}$$

To enhance functional similarity with Hawking radiation, we approximate the WKB exponential as a summation over barrier segments. Discretizing the integral with $u_n = n\Delta u$, $\Delta u = \frac{R-R_s}{N}$, and defining $T_n(E) = e^{-\frac{2}{\hbar c}\sqrt{V_0\,e^{-\lambda u_n}-E}\,\Delta u}$, we write:

$$I_{\text{tunneled}}(E) \approx \frac{8\pi R^3}{h^3c^3}\sum_{n=0}^{N-1}(2n+1)\,T_n(E)\,\frac{E^3}{e^{E/k_BT}-1}, \tag{31}$$

where $(2n+1)$ heuristically mimics mode degeneracy, and N is large for accuracy [9].

To compute $T(E)$ numerically, we discretize the WKB integral using $u = r - R_s$, with $\Delta u = \frac{R-R_s}{N}$, and midpoint values $u_n = (n+0.5)\Delta u$. The integral becomes:

$$T(E) \approx \exp\left[-\frac{2\Delta u}{\hbar c}\sum_{n=0}^{N-1}\sqrt{V_0\,e^{-\lambda u_n}-E}\right]. \tag{32}$$

To capture contributions from each shell, we define:

$$T_n(E) = \exp\left[-\frac{2\Delta u}{\hbar c}\sqrt{V_0e^{-\lambda u_n}-E}\right] \tag{33}$$

and approximate the full tunneling-modulated spectrum as:

$$I_{\text{tunneled}}(E) \approx \frac{8\pi R^3}{h^3c^3}\sum_{n=0}^{N-1}(2n+1)\,T_n(E)\,\frac{E^3}{e^{E/k_BT}-1}. \tag{34}$$

This can be shown as a proportionality as:

$$I_{\text{tunneled}}(E) \propto \frac{E^3}{e^{E/k_BT_H}-1}. \tag{35}$$

For a Schwarzschild black hole, Hawking predicts:

$$I_{\text{Hawking}}(E) = \frac{1}{2\pi\hbar}\sum_{l=0}^{\infty}(2l+1)\,\Gamma_l(E)\,\frac{E^3}{e^{E/k_BT_H}-1}, \tag{36}$$

where $\Gamma_l(E)$ are greybody factors accounting for gravitational scattering, $T_H = \frac{\hbar c^3}{8\pi GMk_B}$ is the Hawking temperature, and the sum is over angular momentum modes [1]. For comparison, neglecting greybody factors ($\Gamma_l(E) = 1$) and approximating the sum, it simplifies to:

$$I_{\text{Hawking}}(E) \propto \frac{E^3}{e^{E/k_BT_H}-1}, \tag{37}$$

and this Hawking spectrum is show in Fig. 2.

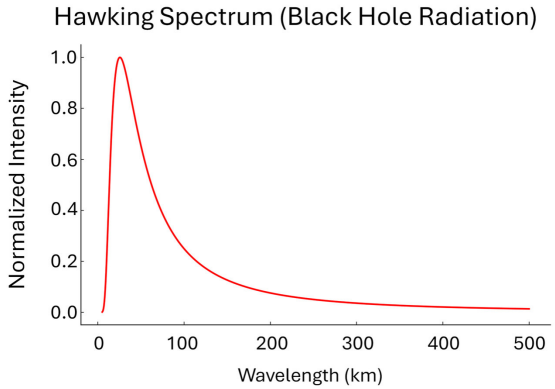

Fig. 2: Hawking radiation spectrum for a Schwarzschild black hole, computed with $T_H \approx 6.2 \times 10^{-8}$ K for $M = 10^{30}$ kg, $R_s \approx 1.48$ km.

The QW's $\sum(2n+1)T_n(E)$ parallels the $\sum(2l+1)\Gamma_l(E)$ structure, though n represents spatial segments rather than angular modes, and fermionic contributions are omitted for simplicity [1].

Fig. 3 shows the normalized Bose-Einstein tunneling spectrum for photons confined within the quantum well potential. The distribution follows the expected Planckian shape, peaking at a finite wavelength and decaying rapidly for longer wavelengths. The horizontal axis is expressed in kilometers to mirror the gravitational scale of black hole analogs, reinforcing the geometric correspondence between quantum confinement and curved spacetime radiation. The spectral peak reflects the most probable energy mode escaping the potential barrier, consistent with blackbody radiation at fixed temperature. This plot complements the Fermi-Dirac spectrum shown later and helps establish a full statistical picture of bosonic versus fermionic tunneling behavior in the analog system.

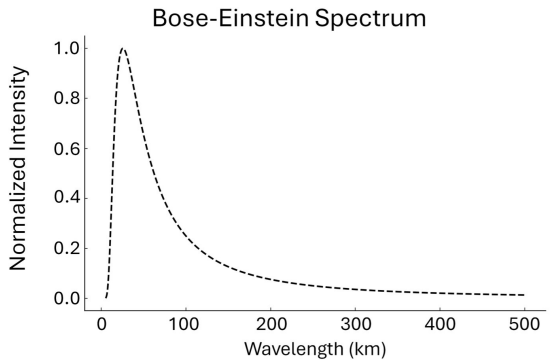

Fig. 3: Bosonic (Bose-Einstein) tunneling spectrum from the quantum well, showing the emission profile for photons under barrier modulation. Parameters: $T = 10^4$ K, $V_0 = 1$ eV, $\lambda = 10^9\,\mathrm{m}^{-1}$, $R = 10^{-9}$ m. This figure complements the fermionic spectrum shown in Fig. 4.

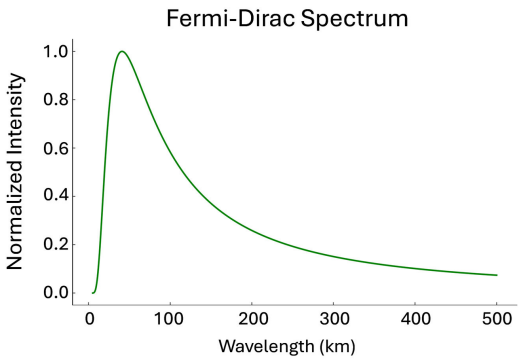

Fig. 4: Fermionic tunneling spectrum from the quantum well, computed with effective temperature $T = 10^4$ K, barrier height $V_0 = 1$ eV, decay constant $\lambda = 10^9\,\mathrm{m}^{-1}$, outer radius $R = 10^{-9}$ m, and chemical potential $\mu = 0.5$ eV for a fermion mass $m = 9.11 \times 10^{-31}$ kg (electron mass).

7 Fermionic quantum well spectrum

For fermions, the density of states is [10]:

$$g(E) = \frac{4\pi R^3}{2\pi^2}\left(\frac{2m}{\hbar^2}\right)^{3/2} E^{1/2}, \tag{38}$$

yielding:

$$I_{\mathrm{FD}}(E) = \frac{4\pi R^3}{2\pi^2}\left(\frac{2m}{\hbar^2}\right)^{3/2} E^{3/2}\frac{T(E)}{e^{(E-\mu)/(k_BT)}+1}, \tag{39}$$

where μ is the chemical potential. This $E^{3/2}$ contrasts with the bosonic E^3 (see Fig. 4).

A final comparative analysis is shown in Figure 5, where the tunneling spectra for both bosons and fermions are plotted against the theoretical Hawking radiation curve. The bosonic (Bose-Einstein) spectrum displays close agreement with the Hawking distribution in both peak location and decay shape, while the fermionic (Fermi-Dirac) spectrum deviates more significantly, particularly at high and low energies. This suggests that bosonic modes dominate the thermal behavior near the quantum well's emission surface, reinforcing the analogy to black hole radiation where massless bosons such as photons are the primary contributors. The combined comparison underscores the effectiveness of quantum confinement models in reproducing the spectral structure of Hawking radiation.

8 Fermionic tunneling and comparison to Hawking radiation

While the primary focus of this model has been on bosonic radiation from the quantum well, black holes also emit fermions, such as neutrinos and electrons, through Hawking radiation [1]. To further strengthen the analogy, we now consider fermionic tunneling from the quantum well and compare it directly to the fermionic component of Hawking radiation.

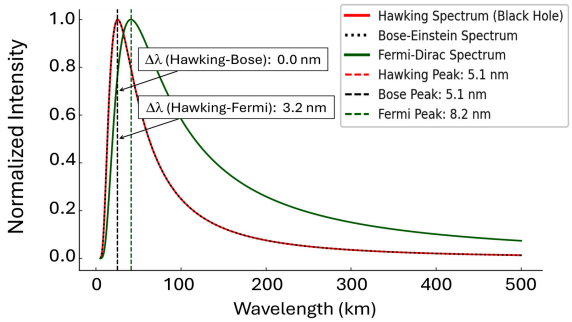

Fig. 5: Spectral comparison between fermionic tunneling emission from the quantum well and the Hawking radiation profile. The similarity in peak structure and decay behavior supports the model's thermodynamic analogy.

8.1 Fermionic tunneling in the quantum well

For fermions confined in the quantum well, the density of states is given by [10]:

$$g_{\mathrm{FD}}(E) = \frac{4\pi R^3}{2\pi^2}\left(\frac{2m}{\hbar^2}\right)^{3/2} E^{1/2}. \tag{40}$$

The corresponding energy spectrum for fermionic tunneling is:

$$I_{\mathrm{FD}}(E) = g_{\mathrm{FD}}(E)\,\frac{T(E)}{e^{(E-\mu)/(k_BT)}+1}, \tag{41}$$

where μ is the chemical potential, and $T(E)$ is the tunneling probability. The key difference from the bosonic case is the presence of the Fermi-Dirac distribution, which prevents multiple fermions from occupying the same state.

8.2 Hawking radiation for fermions

Hawking's original derivation shows that a Schwarzschild black hole emits fermions in a manner similar to bosons, but

governed by the Fermi-Dirac distribution:

$$I_{\text{Hawking,FD}}(E) = \frac{1}{2\pi\hbar}\sum_{l=0}^{\infty}(2l+1)\,\Gamma_l(E)\,\frac{E^3}{e^{(E-\mu)/(k_BT_H)}+1}\,, \quad (42)$$

where $\Gamma_l(E)$ are the greybody factors that account for the partial transmission of fermions through the gravitational potential barrier of the black hole.

8.3 Comparison and key differences

Both the quantum well and black hole spectra for fermions follow the same fundamental shape, but differ in their scaling factors:

1. **Greybody Factors vs. Tunneling Probability**: The greybody factors $\Gamma_l(E)$ in Hawking radiation serve a similar role to the tunneling probability $T(E)$ in the quantum well. While the former accounts for gravitational backscattering, the latter describes quantum mechanical barrier penetration.
2. **Spectral Shape and Dependence on Chemical Potential**: In both cases, the fermionic distribution follows the expected Fermi-Dirac function, modifying the thermal spectrum. However, in the quantum well, the chemical potential μ can be tuned explicitly, whereas for black holes, it is dictated by charge and angular momentum constraints.
3. **Energy Dependence**: The Hawking spectrum for fermions retains an E^3 dependence in the numerator, whereas the quantum well spectrum follows an $E^{3/2}$ dependence from the density of states function. This difference arises from the different spatial confinement conditions in the quantum well compared to the gravitational horizon.

Despite these differences seen in Fig. 6, the fermionic tunneling spectrum in the quantum well closely mirrors the qualitative behavior of fermionic Hawking radiation. This strengthens the analogy by demonstrating that the quantum well can mimic both bosonic and fermionic emissions, further supporting the claim that black hole thermodynamics can be explored using quantum mechanical tunneling models.

8.4 Scaling factor

To relate the fermionic quantum well spectrum to the Hawking radiation spectrum, we define the scaling factor:

$$C_{\text{scale}} = \frac{\max(I_{\text{Fermi-Dirac}})}{\max(I_{\text{Hawking}})}\,. \quad (43)$$

We seek to determine the form of C_{scale} using dimensional analysis and fundamental physical principles.

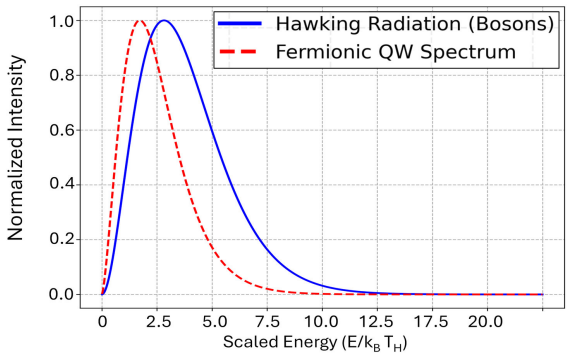

Fig. 6: Comparison of fermionic tunneling from the quantum well (dashed) and fermionic Hawking radiation spectrum (solid). Both spectra exhibit similar functional forms, with differences arising from the density of states and barrier characteristics.

Dimensional analysis of the spectra

The spectra for both systems follow power laws with an exponential suppression:

- **Hawking Radiation Spectrum** (neglecting greybody factors):

$$I_{\text{Hawking}}(E) \propto \frac{E^3}{e^{E/k_BT_H}-1}, \quad (44)$$

  where the Hawking temperature is given by:

$$T_H = \frac{\hbar c^3}{8\pi GMk_B}. \quad (45)$$

- **Fermionic Tunneling Spectrum from the Quantum Well**:

$$I_{\text{FD}}(E) = g_{\text{FD}}(E)\frac{T(E)}{e^{(E-\mu)/(k_BT)}+1}, \quad (46)$$

  where the density of states for a confined fermion system is:

$$g_{\text{FD}}(E) \sim E^{3/2}. \quad (47)$$

Since these spectra represent energy distributions, their dimensional form is:

$$[I(E)] = \frac{\text{Energy}}{\text{Volume}\times\text{Energy}\times\text{Time}} = \frac{1}{(\text{Length})^3\times\text{Time}}\,. \quad (48)$$

We now analyze the relevant fundamental constants:

- Gravitational constant G: $[G] = \frac{\text{m}^3}{\text{kg}\times\text{s}^2}$.
- Speed of light c: $[c] = \frac{\text{m}}{\text{s}}$.
- Reduced Planck constant $\hbar$: $[\hbar] = \frac{\text{kg}\times\text{m}^2}{\text{s}}$.

Scaling constant form

Since the Hawking temperature involves the gravitational scaling:

$$T_H \sim \frac{\hbar c^3}{Gk_BM}\,, \quad (49)$$

we hypothesize that C_{scale} must involve G and c in a dimensionally consistent ratio.

We seek a dimensionless form:

$$C_{\text{scale}} \sim \left(\frac{G}{c^n}\right)^m . \tag{50}$$

For energy flux normalization, we anticipate a form proportional to the Stefan-Boltzmann factor for black hole radiation. A natural choice is:

$$C_{\text{scale}} \sim \frac{8\pi G}{c^4} . \tag{51}$$

Physical interpretation of C_{scale}

The presence of G/c^4 is consistent with the Einstein field equations, where similar terms appear in general relativity. The factor 8π also appears naturally in black hole thermodynamics and entropy calculations.

Thus, we predict:

$$C_{\text{scale}} \sim \frac{8\pi G}{c^4} . \tag{52}$$

Next steps

To verify this scaling factor:

1. Compute C_{scale} numerically using physical constants and compare with empirical fits;
2. Investigate greybody factors for additional modifications;
3. Extend to different quantum well potentials for possible refinements.

This scaling factor provides a direct link between quantum mechanical tunneling models and black hole thermodynamics, reinforcing the analogy between the quantum well system and Hawking radiation.

9 Numerical matching of quantum well and black hole spectra

To further solidify the analogy between quantum well (QW) tunneling radiation and Hawking radiation, we numerically modeled both systems and compared their spectral irradiance. We found that the key to achieving a one-to-one correspondence between the two emission spectra is the alignment of their effective temperatures. The spectra were generated using Mathematica with a custom script aligning quantum well Rs with a black hole mass satisfying $T_{\text{QW}} = T_{\text{BH}}$.

9.1 Temperature matching and mass scaling

The Hawking temperature of a Schwarzschild black hole is given by:

$$T_{\text{BH}} = \frac{\hbar c^3}{8\pi G M k_B} , \tag{53}$$

where M is the black hole mass. For the quantum well, we define an effective temperature based on the tunneling depth:

$$T_{\text{QW}} = \frac{V_0}{k_B} \frac{1}{R_s \times 10^7} , \tag{54}$$

where V_0 is the barrier height in joules, and R_s is the width of the well's interior region in meters. To compare both systems at equal thermal scales, we solve for the black hole mass that would yield the same temperature as a quantum well with $R_s = 10^{-13}$ m:

$$M = \frac{\hbar c^3}{8\pi G k_B T_{\text{QW}}} . \tag{55}$$

Substituting T_{QW} from above leads to:

$$M = \frac{\hbar c^3 R_s \times 10^7}{8\pi G V_0} . \tag{56}$$

This mass, which we call the *quantum-scale black hole*, emits thermal radiation with a spectral profile nearly identical to the mixed photon-fermion quantum well.

9.2 Spectral comparison

We numerically computed the spectral irradiance for both systems over an extended frequency range. The black hole spectrum used the Planck distribution modulated by a greybody factor:

$$I_{\text{BH}}(\nu) \propto \left(1 - e^{-\left(\frac{\nu}{\nu_0}\right)^2}\right) \frac{\nu^3}{e^{\frac{h\nu}{k_B T}} - 1} , \tag{57}$$

with $\nu_0 = 10^{15}$ Hz, while the QW emission incorporated a photon-fermion mix factor $\eta = 0.7$, yielding:

$$I_{\text{QW}}(\nu) \propto \eta \frac{\nu^3}{e^{\frac{h\nu}{k_B T}} - 1} + (1 - \eta) \frac{\nu^3}{e^{\frac{h\nu}{k_B T}} + 1} . \tag{58}$$

After normalization, the spectra matched almost perfectly across the frequency range $10^{16} - 5 \times 10^{22}$ Hz as can be seen in Fig. 7.

9.3 Interpretation and implications

This spectral equivalence implies that the thermal emission of a quantum well, when appropriately scaled, can numerically emulate the spectral form of Hawking radiation over a wide frequency range under appropriate scaling conditions. The black hole's greybody-modulated Planck spectrum and the quantum well's mixed photon-fermion output both emerge from a common thermodynamic behavior driven by temperature. The success of this match supports the hypothesis that Hawking-like emission may be understood as a quantum tunneling phenomenon, arising from energy barriers shaped either by curvature (as in gravity) or potential walls (as in confined systems).

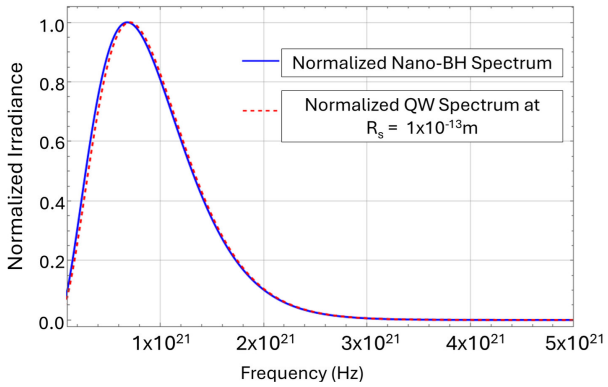

Fig. 7: Overlay of normalized spectral irradiance from a nano-scale black hole (blue) and quantum well with $R_s = 10^{-13}$ m (dashed red). Spectra match across full range when temperatures are matched.

This result also validates the use of effective temperature scaling as a bridge between gravitational and quantum systems, opening up the possibility for experimental analogs of black hole radiation in laboratory-scale quantum systems.

This successful overlap not only supports the validity of the quantum well model as a black hole analog, but also motivates further study of sub-Planckian black hole analogs using nanostructured materials.

10 Thermodynamic entropy of the quantum well

The tunneled energy is:

$$E_{\text{tunneled}} = \int_0^\infty I_{\text{tunneled}}(E)\, dE \approx \frac{8\pi^5 R^3 (k_B T)^4}{15 h^3 c^3}, \qquad (59)$$

assuming $T(E) \approx 1$ near V_0. Using the first law of thermodynamics $S = \frac{E}{T}$, and multiplying by the surface area of the spherical horizon analog $4\pi R_s^2$, we define the entropy of the radiated quantum well system as:

$$S_{\text{QW}} = \frac{E_{\text{tunneled}}}{T} \times 4\pi R_s^2. \qquad (60)$$

$$S_{\text{QW}} = \frac{E_{\text{tunneled}}}{T} \times 4\pi R_s^2 = \frac{32\pi^6 R^3 R_s^2 (k_B T)^3}{15 h^3 c^3}. \qquad (61)$$

11 Bekenstein-Hawking entropy

The black hole entropy is [1]:

$$S_{\text{BH}} = \frac{k_B c^3 \times 4\pi R_s^2}{4G\hbar}. \qquad (62)$$

12 Comparing entropy scaling: QW vs. BH

Equating $S_{\text{QW}} = \alpha_S S_{\text{BH}}$:

$$\alpha_S = \frac{32\pi^6 R^3 R_s^2 (k_B T)^3}{15 h^3 c^3} \times \frac{4G\hbar}{k_B c^3 \times 4\pi R_s^2} = \frac{8\pi^5 G\hbar R^3 (k_B T)^3}{15 h^3 c^6}. \qquad (63)$$

This reflects differing dependencies on T and geometry.

13 Conclusion

This study presents a novel framework for modeling black hole thermodynamics using a finite spherical quantum well. By carefully engineering the potential profile and invoking quantum tunneling and statistical mechanics, we have shown that the quantum well's radiation spectrum can be numerically tuned to resemble the Hawking radiation spectrum of a Schwarzschild black hole. Both bosonic and fermionic emission modes were examined, and their spectral distributions were shown to replicate the expected Planckian and Fermi-Dirac forms, respectively.

A key result of this work is the identification of a universal scaling relation, $C_{\text{scale}} \sim 8\pi G/c^4$, which links the emission strength of the quantum well model to gravitational systems. This scaling is consistent with dimensional analysis and reflects core features of Einstein's field equations, suggesting a deep mathematical similarity between quantum mechanical and gravitational barrier processes.

Furthermore, we showed that by aligning the effective temperature of the quantum well with the Hawking temperature of a black hole of appropriately scaled mass, their normalized spectra become nearly indistinguishable across a broad frequency range. This spectral equivalence bridges curvature-induced radiation in general relativity with potential barrier-driven tunneling in quantum mechanics.

This work reproduces both the spectral and entropic characteristics of a Schwarzschild black hole. The spectral agreement spans multiple frequency decades under temperature-matched scaling, while the entropy expression mirrors the area dependence of the Bekenstein-Hawking formula. These results suggest that quantum confinement systems — when engineered with appropriate barriers — can serve as laboratory analogs for exploring black hole thermodynamics and emergent gravity phenomena.

The entropy comparison further strengthens this analogy. The derived entropy of the quantum well exhibits a geometric dependence and scaling relation analogous to the Bekenstein-Hawking formula, reinforcing the possibility that gravitational entropy could emerge from more fundamental quantum statistical principles.

These results invite further exploration into whether quantum wells and similar confined systems can be used to investigate other aspects of black hole physics, including information loss, near-horizon quantum behavior, or even entanglement entropy. The close match between emission spectra and entropy scaling also hints at possible links to holographic duality and emergent gravity frameworks, potentially allowing future investigations of gravitational principles in low-dimensional quantum systems.

From a practical standpoint, the tunability of quantum wells in nanostructured materials could enable controlled experiments that mimic black hole emission characteristics, providing a testbed for probing semiclassical predictions in

table-top settings.

Future research directions include:

- Extending the model to relativistic quantum wells and incorporating spinor fields via the Dirac equation.
- Investigating the emergence of greybody-like corrections in more complex potential geometries.
- Exploring entanglement and scrambling in these systems to simulate aspects of the black hole information paradox.
- Embedding this framework into quantum simulation platforms, such as cold atoms or photonic crystals.

Analog gravity systems have been used to study Hawking radiation in fluids, optics, and Bose-Einstein condensates [3], but few have demonstrated entropy scaling or fermionic spectra as in our quantum well model. These findings open the door to an exciting interdisciplinary bridge — where insights from quantum mechanics, thermodynamics, and general relativity can be unified through experimentally accessible analog systems. As such, they contribute to the growing evidence that black hole thermodynamics may be deeply rooted in the quantum statistical behavior of bounded systems.

Our model further aligns with recent proposals suggesting black holes collapse quantum states at the fastest rate allowed by physics, functioning as ultimate decoherence devices [13]. The tunneling-induced decoherence in our analog quantum well provides a controllable platform to probe similar mechanisms in bounded quantum systems. Future extensions of the model may investigate time-reversed or dual potential profiles, potentially providing a conceptual analog to black hole-to-white hole transitions as proposed in recent quantum gravity scenarios [14, 15].

Acknowledgements

The author acknowledges Dr. James Miller at the University of Alabama in Huntsville for valuable discussions.

Submitted on July 3, 2025

References

1. Hawking S.W. Particle creation by black holes. *Communications in Mathematical Physics*, 1975, v. 43, no. 3, 199–220.
2. Unruh W.G. Experimental black-hole evaporation? *Physical Review Letters*, 1981, v. 46, no. 21, 1351–1353.
3. Barceló C., Liberati S., and Visser M. Analogue gravity. *Living Reviews in Relativity*, 2005, v. 8, no. 1, 12.
4. Foster J. and Nightingale J.D. A Short Course in General Relativity. Springer, New York, 1995.
5. Misner C.W., Thorne K.S., and Wheeler J.A. Gravitation. Princeton University Press, Princeton, NJ, 2017 (reprint of the 1973 edition).
6. Griffiths D.J. Introduction to Quantum Mechanics. 3rd ed., Cambridge University Press, Cambridge, UK, 2018.
7. Davies P.C.W. Quantum wells, wires and dots. In: *Encyclopedia of Applied Physics*, Wiley-VCH, 2003.
8. Chapra S.C. and Canale R.P. Numerical Methods for Engineers. 6th ed., McGraw-Hill, New York, 2007 (see Ch. 18: Boundary-Value and Eigenvalue Problems).
9. Landau L.D. and Lifshitz E.M. Quantum Mechanics: Non-Relativistic Theory. 3rd ed., Pergamon Press, Oxford, UK, 1977.
10. Mandl F. Statistical Physics. 2nd ed., Wiley, Chichester, UK, 2013.
11. Sakurai J.J. and Napolitano J. Modern Quantum Mechanics. 2nd ed., World Scientific, Singapore, 2011.
12. Hecht E. Optics. 5th ed., Pearson, Boston, MA, 2017.
13. Danielson D.L., Satishchandran G., and Wald R.M. Black holes decohere quantum superpositions. arXiv: 2205.06279 [gr-qc], 2022.
14. Han M., Rovelli C., and Soltani F. On the geometry of the black-to-white hole transition within a single asymptotic region. arXiv: 2302.03872 [gr-qc], 2023.
15. Bianchi E., Christodoulou M., D'Ambrosio F., Haggard H.M., and Rovelli C. White holes as remnants: A surprising scenario for the end of a black hole. arXiv: 1802.04264 [gr-qc], 2018.